

Electronic Supplementary Information (ESI)

$\text{Cu}_2\text{ZnSnS}_4$ and $\text{Cu}_2\text{ZnSn}(\text{S}_{1-x}\text{Se}_x)_4$ nanocrystals: room-temperature synthesis and efficient photoelectrochemical water splitting

Jun Xu,^{*a} Zhengqiao Hu,^a Junjun Zhang,^b Wei Xiong^b, Lianling Sun,^a Lei Wan,^d Ru Zhou,^d Yang Jiang^c and Chun-Sing Lee^{*b}

^aSchool of Electronic Science & Applied Physics, Hefei University of Technology, Hefei 230009, P. R. China

^bCenter of Super-Diamond and Advanced Films (COSDAF), and Department of Chemistry, City University of Hong Kong, Hong Kong SAR, P. R. China

^cSchool of Materials Science and Engineering, Hefei University of Technology, Hefei 230009, P. R. China

^dSchool of Electrical Engineering and Automation, Hefei University of Technology, Hefei 230009, P. R. China

*E-mail: apjunxu@hfut.edu.cn (J. Xu), apcslee@cityu.edu.hk (C.S. Lee)

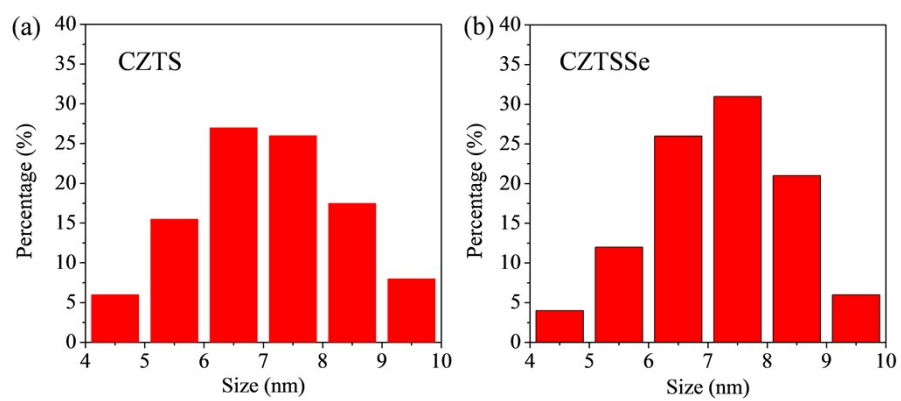


Fig. S1 Size distribution maps of the CZTS and CZTSSe nanocrystals.

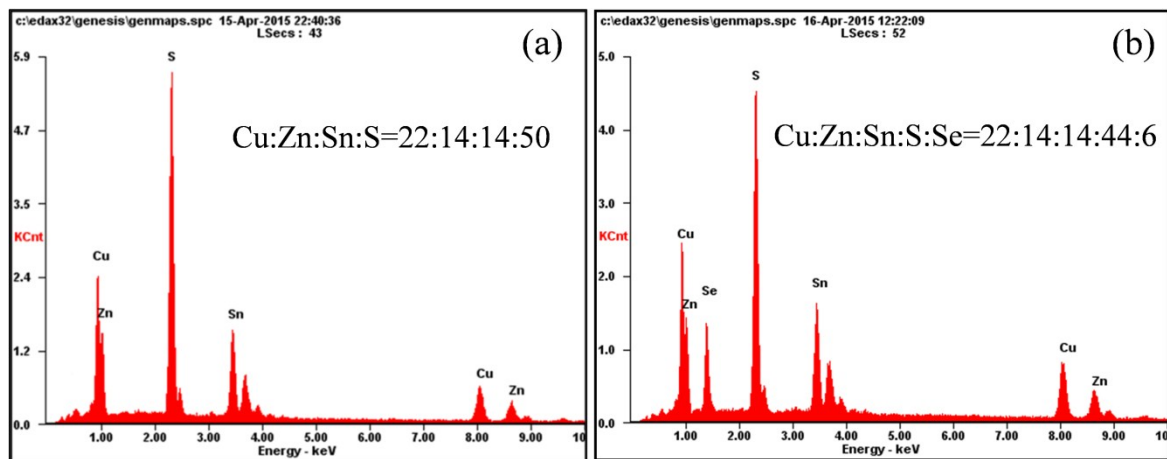


Fig. S2 EDX spectra of (a) the CZTS nanocrystals and (b) the CZTSSe nanocrystals.

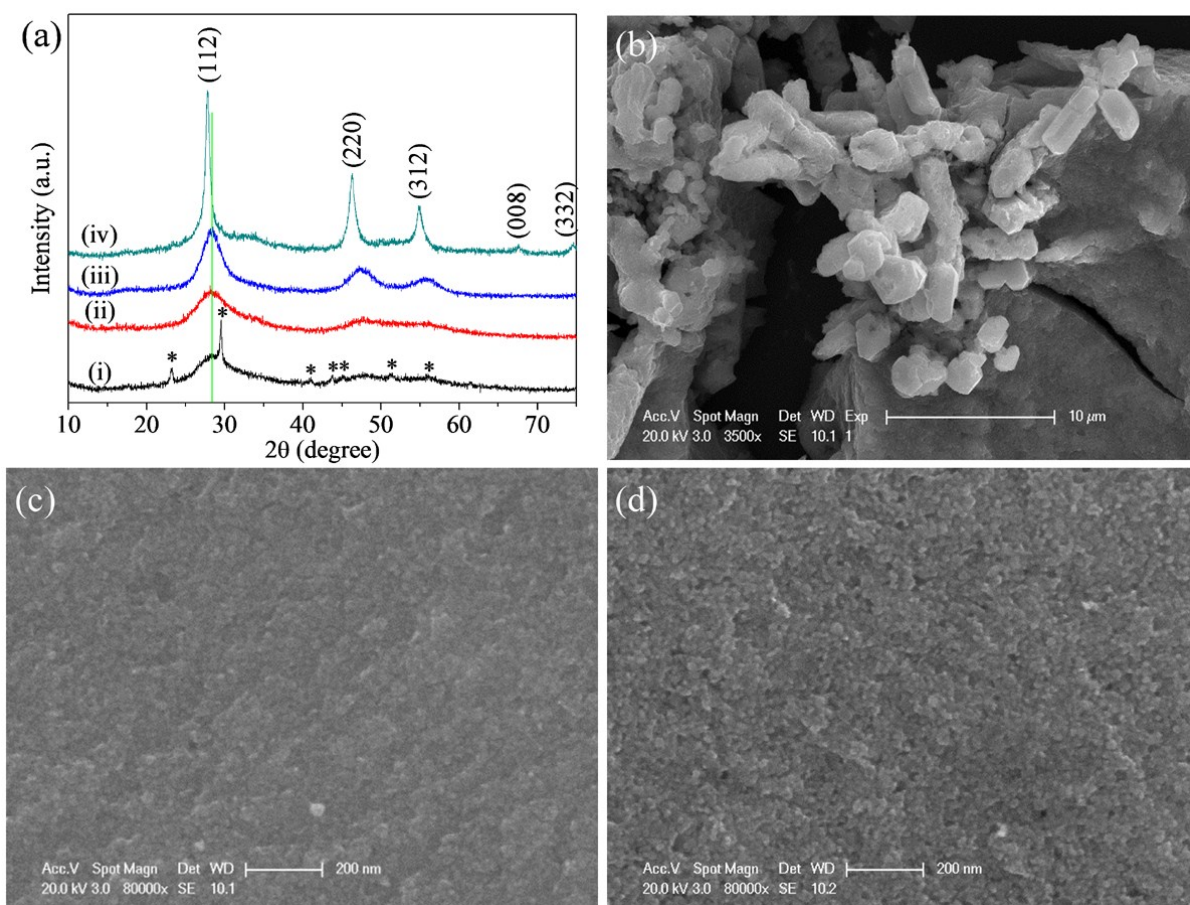


Fig. S3 (a) XRD patterns of (i) the as-prepared CZTSSe nanocrystals without purification, the peaks marked with * correspond to Se (JCPDF No. 86-2246), (ii) the CZTSSe nanocrystals after purification by post-treatment in the NaBH_4 solution, (iii) the unpurified CZTSSe sample annealed at 200 °C, (iv) the unpurified CZTSSe sample annealed at 400 °C, the shift of (112) peak is due to selenization by the Se by-product. (b) An SEM image of the unpurified CZTSSe nanocrystals, showing the existence of Se microrods. (c) An SEM image of the CZTSSe nanocrystals after purification by post-treatment in a NaBH_4 solution. (d) An SEM image of the CZTSSe nanocrystals after annealing in nitrogen flow at 400 °C.

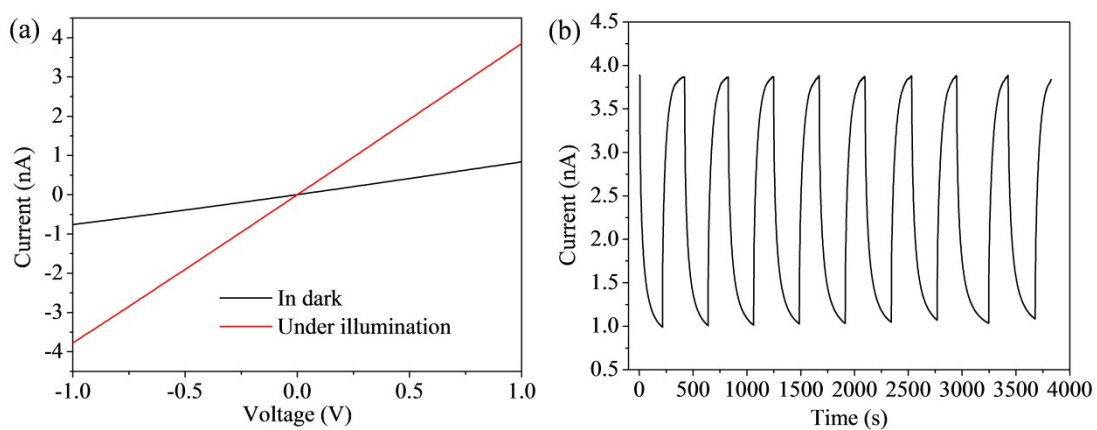


Fig. S4 (a) I-V curves of the CZTS nanocrystal film on a glass substrate in the dark and under AM 1.5G illumination at an intensity of 100 mW cm^{-2} ; (b) Time-resolved photoresponse of the CZTS nanocrystal film at a bias of 1.0 V.

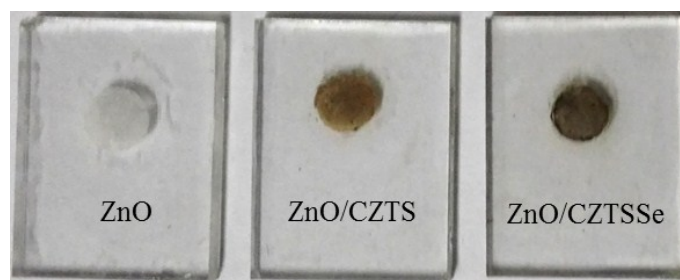


Fig. S5 Photographs of the ZnO, ZnO/CZTS, ZnO/CZTSSe photoanodes.

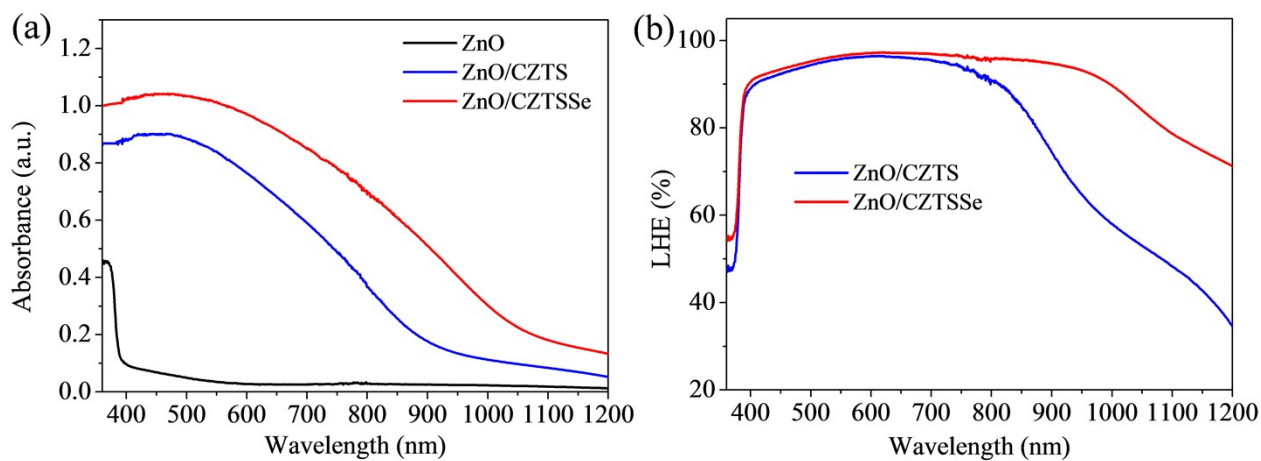


Fig. S6 (a) UV-vis absorption spectra of the various photoanodes; (b) LHE of the ZnO/CZTSSe and ZnO/CZTS photoanodes. Calculation of LHE can be referred to references (Energy Environ. Sci. 2012, 5, 8896; Electrochim. Acta 2016, 191, 62).

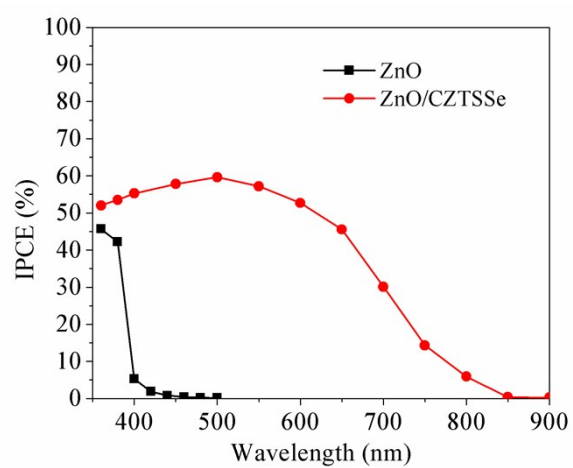


Fig. S7 IPCE spectra of the ZnO/CZTSSe and the bare ZnO photoanodes at a bias of 1.23 V vs NHE.

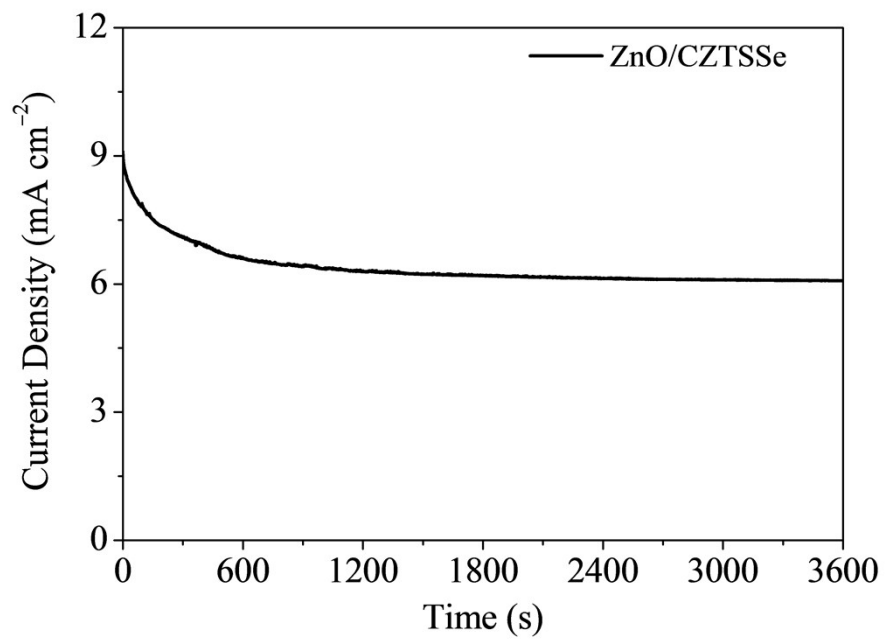


Fig. S8 Time-resolved photocurrent of the ZnO/CZTSSe photoanode.

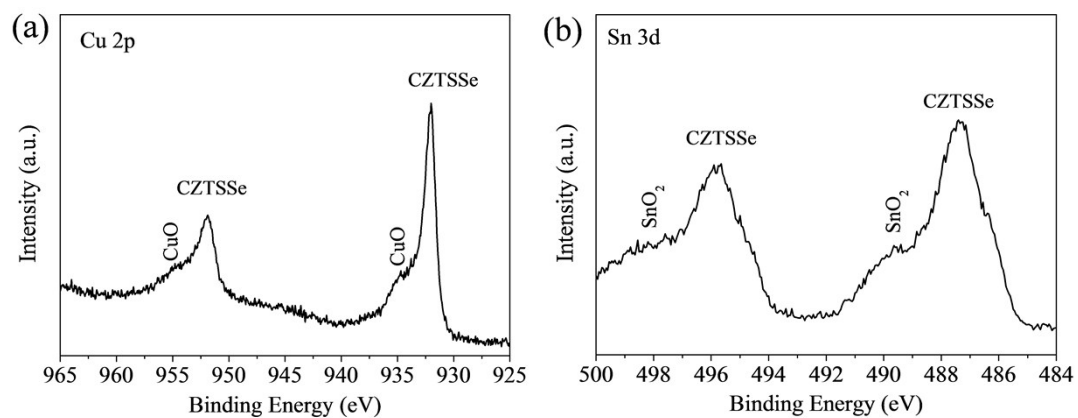


Fig. S9 XPS spectra of Cu 2p and Sn 3d from the ZnO/CZTSSe sample after stability test.